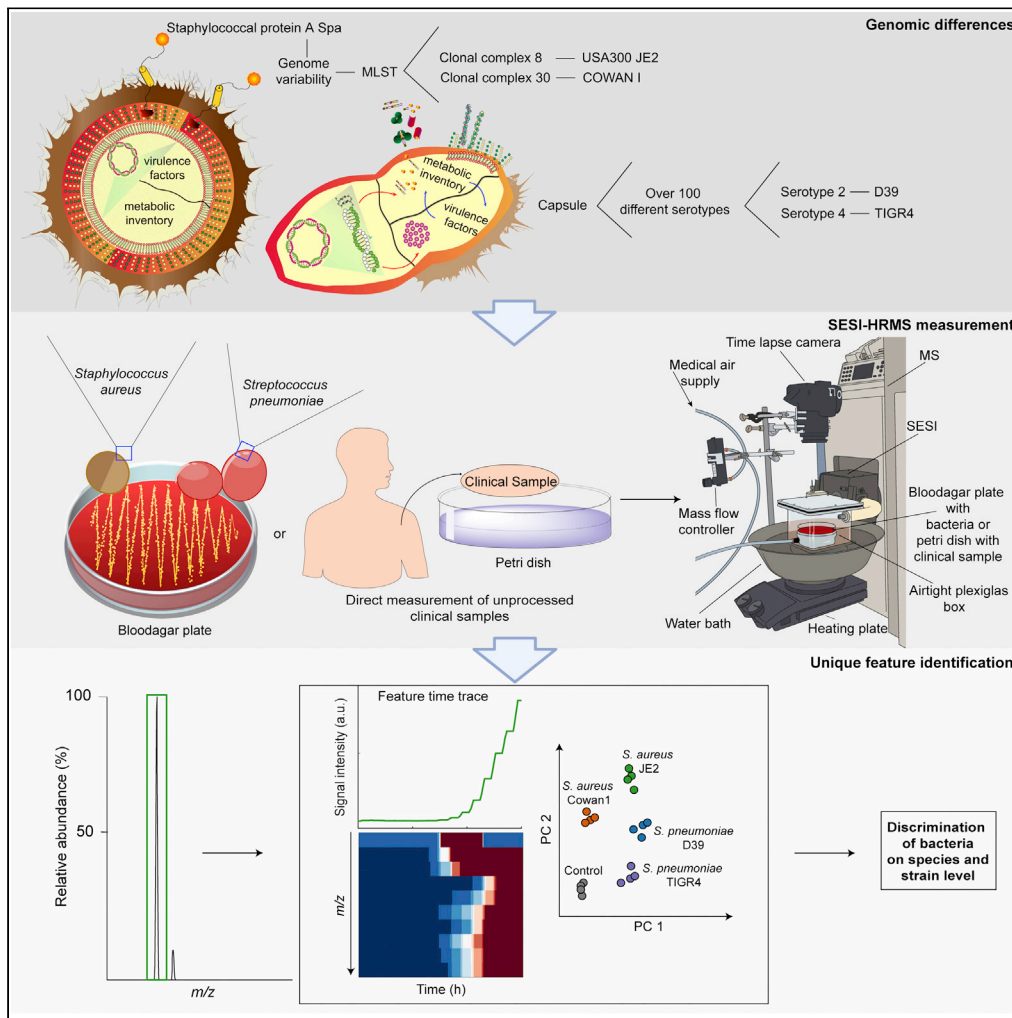


Article

Rapid detection of *Staphylococcus aureus* and *Streptococcus pneumoniae* by real-time analysis of volatile metabolites



Alejandro Gómez-Mejia, Kim Arnold, Julian Bär, ..., Silvio D. Brugger, Annelies S. Zinkernagel, Pablo Sinues

annelies.zinkernagel@usz.ch (A.S.Z.)
pablo.sinues@unibas.ch (P.S.)

Highlights

Real-time mass spectrometry shows potential as a tool for microbiological diagnosis

Bacterial volatile metabolites from 1×10^3 CFUs are detected within minutes

S. aureus and *S. pneumoniae* can be distinguished on species and even strain level

Complex clinical samples cluster according to presence or absence of viable bacteria



Article

Rapid detection of *Staphylococcus aureus* and *Streptococcus pneumoniae* by real-time analysis of volatile metabolites

Alejandro Gómez-Mejía,^{1,4} Kim Arnold,^{2,3,4} Julian Bär,¹ Kapil Dev Singh,^{2,3} Thomas C. Scheier,¹ Silvio D. Brugger,¹ Annelies S. Zinkernagel,^{1,5,*} and Pablo Sinues^{2,3,5,6,*}

SUMMARY

Early detection of pathogenic bacteria is needed for rapid diagnostics allowing adequate and timely treatment of infections. In this study, we show that secondary electrospray ionization–high resolution mass spectrometry (SESI-HRMS) can be used as a diagnostic tool for rapid detection of bacterial infections as a supportive system for current state-of-the-art diagnostics. Volatile organic compounds (VOCs) produced by growing *S. aureus* or *S. pneumoniae* cultures on blood agar plates were detected within minutes and allowed for the distinction of these two bacteria on a species and even strain level within hours. Furthermore, we obtained a fingerprint of clinical patient samples within minutes of measurement and predominantly observed a separation of samples containing live bacteria compared to samples with no bacterial growth. Further development of this technique may reduce the time required for microbiological diagnosis and should help to improve patient’s tailored treatment.

INTRODUCTION

A prompt and accurate identification of the causative pathogens of a bacterial infection is essential for providing patients with adequate treatments to reduce mortality and to prevent antibiotic resistance (Kumar et al., 2006; Lodise et al., 2003; Paul et al., 2010; Rasmussen et al., 2010). Bacterial infections caused by the human pathogenic bacteria *Staphylococcus aureus* and *Streptococcus pneumoniae* remain highly prevalent (Choi et al., 2021; Henriques-Normark and Normark, 2010; Kyaw et al., 2005; Lowy, 1998). Despite the development and availability of antibiotics, mortality remains high, reaching 20 % for *S. aureus*-associated endocarditis and more than one million deaths of children below 5 years of age by *S. pneumoniae* (Choi et al., 2021; Henriques-Normark and Normark, 2010).

Currently, state-of-the-art bacterial identification methods consist of different strategies: in addition to conventional growth-based diagnostics, molecular methods (16S-rRNA, whole genome sequencing and antigen detection) and matrix-assisted laser desorption/ionization time-of-flight (MALDI-TOF) mass spectrometry are the current culture-based gold standards for identification of bacteria (Griffiths, 2008; Vandamme et al., 1996; Vrioni et al., 2018; Yarza et al., 2014). Both methods portray complementary properties. Molecular methods allow for detection of single bacterial components such as pneumococcal antigen or DNA directly in a clinical sample. This translates into a similar diagnostic tool comparable to MALDI-TOF at the cost of not being able to differentiate between live and dead bacteria or to present limitations to identify antibiotic susceptibilities (Opota et al., 2015). On the other hand, the rich peptide fingerprints detected by MALDI-TOF allow for a very high degree of specificity, covering a vast range of pathogens. However, this gold-standard method still bears limitations. In order to be able to identify a bacterium, a minimum concentration of bacteria must be grown for a defined time to allow an accurate identification of the sample (Cheng et al., 2018; Clark et al., 2018; Griffiths, 2008; Singhal et al., 2015; Vrioni et al., 2018). Such prerequisite introduces additional time for diagnosis of approximately 16 to 24 h until the bacteria have grown sufficiently (Altun et al., 2015; Buchan et al., 2012; Clark Andrew et al., 2013). Studies in the last decade have aimed to reduce the time required for MALDI-TOF preprocessing, with diverse ranges of success from 3 to 5 h turnover; however, this also implied a reduction in the specificity of the results (Altun et al., 2015; Nomura et al., 2020).

¹Department of Infectious Diseases and Hospital Epidemiology, University Hospital Zurich, University of Zurich, 8091 Zurich, Switzerland

²University Children’s Hospital Basel (UKBB), 4056 Basel, Switzerland

³Department of Biomedical Engineering, University of Basel, 4123 Allschwil, Switzerland

⁴These authors contributed equally

⁵These authors contributed equally

⁶Lead contact

*Correspondence: annelies.zinkernagel@usz.ch (A.S.Z.), pablo.sinues@unibas.ch (P.S.)
<https://doi.org/10.1016/j.isci.2022.105080>



Additional experimental methods are being developed to overcome these limitations of the techniques currently accepted in microbiological diagnostics. One approach is to detect volatile metabolites (i.e. volatile organic compounds aka VOCs) released by microorganisms as they grow (Bos et al., 2013; Sethi et al., 2013). The development of “electronic noses” in the early 1980s and its utilization for bacteria detection in clinical diagnosis and the food industry showcased the importance of volatile analysis and further increased the development of related technologies (Casalinuovo et al., 2006; Gardner and Bartlett, 1994). An additional approach has also been taken by selected-ion flow-tube mass spectrometry (SIFT-MS) where one study reported the detection of different bloodborne pathogens such as *S. aureus*, *S. pneumoniae*, and *P. aeruginosa* after 6 h of incubation in special blood enrichment media, leading to the feasibility of a fast detection of bacterial pathogens directly from cultures, albeit requiring high concentrations of bacteria (Allardyce et al., 2006a; Allardyce et al., 2006b). Furthermore, additional technologies such as ion mobility spectrometry (IMS) has also been applied to analyze bacterial culture *in vitro* as well as patients’ breath to generate correlations within patients presenting ongoing bacterial infections, such as tuberculosis with a sensitivity of 81% (Sahota et al., 2016; Steppert et al., 2021). Moreover, the IMS technology coupled to gas chromatography has also been applied successfully to analyze bacterial growth derived from blood by enriching its bacterial content (Drees et al., 2019). By doing so, the limitations of molecular methods such as time to positive detection and distinguishing between dead and live bacteria are overcome. In addition, similarly to the specificity provided by the peptide profiles captured by MALDI-TOF, the unique metabolism developed over millions of years of evolution of bacteria provides an opportunity to render a high specificity. This strategy has been usually pursued by different mass spectrometric variants. The workhorse of VOCs analysis released by bacteria has been gas chromatography-mass spectrometry (GC-MS) possessing the main advantage to detect very complex gas mixtures (Bean et al., 2012). However, this method requires time-consuming sample preparation, limiting the possibilities of providing quicker results than MALDI-TOF-based analyses. Alternative real-time mass spectrometric techniques such as SIFT-MS and secondary electrospray ionization–high resolution mass spectrometry (SESI-HRMS) (Ballabio et al., 2014; Bean et al., 2014; Kaeslin et al., 2021; Lee and Zhu, 2020; Li et al., 2019; Li and Zhu, 2018; Zhu et al., 2010, 2013a, 2013b, 2013c; Zhu and Hill, 2013) can provide analyses of VOCs on the fly, thus potentially shortening time-to-results.

Despite the encouraging results and evidence accumulated over decades of analysis of VOCs released by pathogens, such analytical strategy did not make it to transition from a research level to a commercially available solution. Some of the reasons include that it is unclear yet whether the sensitivity of such methods is enough to detect bacterial growth during very early stages of bacterial replication, hence potentially accelerating positive results to just a few hours. Another remaining question is whether at such low VOCs concentration levels, the selectivity is enough to enable species differentiation. In this work, we addressed these open questions using SESI-HRMS, which features limits of detection for VOC features as low as part-per-trillion (Martinez-Lozano et al., 2009) and operates in real time. Additionally, SESI-HRMS allows for the simultaneous detection of hundreds of VOCs from microorganisms because of the high resolution of the mass analyzer (Tejero Rioseras et al., 2017). To do so, we conducted quantitative measurements of two different *S. aureus* and *S. pneumoniae* strains. Parallel image analysis and gold-standard culture and MALDI-TOF measurements were used to benchmark the technology. Previous studies have sought to directly measure *in vitro* and *ex vivo* volatile molecules from a diverse set of clinical samples (wound swabs, tissue, body fluids, among others) using gas sensors and mass spectrometry-based technologies (Allardyce et al., 2006b; Byun et al., 2010; Daulton et al., 2020; Ratiu et al., 2019; Roine et al., 2014; Slade et al., 2017; Thomas et al., 2010); with this in mind, we culminated the study providing proof-of-principle on the feasibility of this sample preparation-free approach to “sniff-out” a variety of clinical samples with high complexity such as unprocessed tissue and prosthetic implants in real time.

RESULTS

Detection and quantification of low-level bacterial colony forming units (CFUs)

To evaluate the capability of SESI-HRMS for the detection of bacterial VOC features, we measured a low number of CFUs (140 – 2000 CFUs per plate) of *S. aureus* and *S. pneumoniae* strains over ~15 h with SESI-HRMS. In parallel, time-lapse (TL) images were acquired to record bacterial growth over 15 h and up to 38 h for certain replicates (Figure 1 and see also Figure S1). As an example, Figure 1A shows a time trace of an unspecific mass spectral feature present in all four biological replicates of *S. aureus* Cowan1 during SESI-HRMS measurement at a mass-to-charge ratio (m/z) 144.04765. Complementary TL pixel intensities for each replicate are presented in Figure 1B, accompanied by control measurements

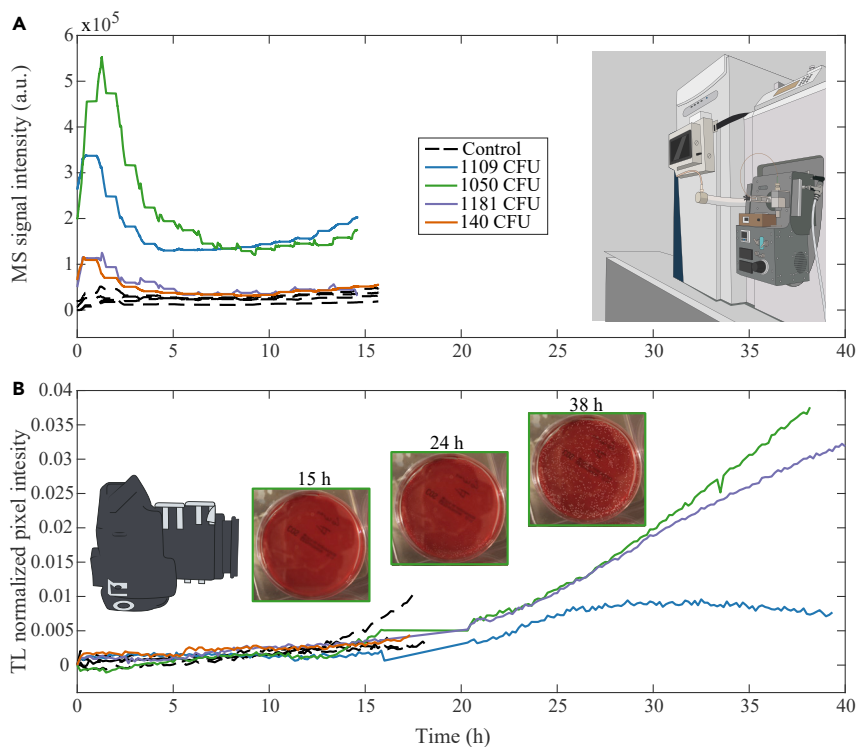


Figure 1. Detection of features in headspace of growing bacterial culture by SESI-HRMS vs. visual monitoring by TL camera

(A) Example of an unspecific feature time trace at m/z 144.04765 with proposed molecular formula $[C_6H_{11}O_2NS]^+$ acquired by SESI-HRMS over 15 h of measurement is illustrated for *S. aureus* Cowan1.

(B) Corresponding TL normalized pixel intensity of the measured replicates along with pictures showing visually captured growth at 15, 24, and 38 h after the bacteria were put on the plate. The four colored lines represent four biological replicates and the four dashed black lines represent the four control replicates. The colors indicate how many CFUs were put on the blood agar plate for each replicate measured. MS=Mass spectrometer, CFU = Colony forming unit, TL = Time lapse. See also [Figure S1](#).

together with TL image row examples at 15, 24, and 38 h of measurement. No bacteria were visually detected by the TL system by the end of SESI-HRMS acquisition at 15 h. In contrast, m/z 144.04765 in *S. aureus* Cowan1 was detected by SESI-HRMS in all four replicates within the first minutes of growth/measurement even if CFU numbers are as low as 140 CFUs ([Figure 1A](#)). To control for bacterial growth, the plates were further analyzed via TL beyond the 15 h analysis with SESI-HRMS, confirming the appearance of colonies after 24 h of growth ([Figure 1B](#)). In general, growth was detected for all bacterial strains under low CFU condition as well as under high CFU condition (see also [Figure S1](#)).

Discrimination ability: Real-time detection of unique features on species and strain level

After confirming the detection of features under a low number of CFUs, we investigated whether these detected features were attributable to the *S. aureus* strains JE2 and Cowan1 or the *S. pneumoniae* strains D39 and TIGR4. We were able to assign a total of 392 features to the two bacterial species or their respective strains as summarized in [Table S1](#). We found that out of 392 features, 51 features were *S. aureus*-specific (JE2 and Cowan1), 302 features were unique to *S. aureus* JE2, and 15 features unique to *S. aureus* Cowan1. Moreover, 18 features were identified as *S. pneumoniae*-specific (D39 and TIGR4), five features were unique to *S. pneumoniae* D39, and one feature was unique to *S. pneumoniae* TIGR4.

Since the features listed in [Table S1](#) identified for low CFUs (in the order of thousands) were not always present in all four biological replicates measured for a bacterial strain, we aimed to evaluate the use of SESI-HRMS with high-density (billions) CFUs cultures to increase the signal strength and achieve a better reproducibility among the four biological replicates measured for each bacterial strain. [Table S2](#) summarizes the total of 1,269 features identified to be unique for a distinct bacterial strain or species under

high-density conditions. Out of the total of 1,269 features, 19 features were detected in both *S. aureus* strains JE2 and Cowan1. Three specific features were only found in *S. aureus* Cowan1 and 26 features in *S. aureus* JE2. For *S. pneumoniae*, 15 specific features were present in both strains D39 and TIGR4. When both *S. pneumoniae* strains were evaluated separately, 1,206 features were unique to *S. pneumoniae* D39 and no unique features were identified for TIGR4.

Out of the 26 features assigned to the strain *S. aureus* JE2, one representative feature at m/z 104.10693 is shown for all biological replicates and the controls (Figure 2A). The signal of this particular feature was more abundant in all four *S. aureus* JE2 replicates with a signal intensity of $\sim 4 \times 10^5$ (a.u.) and nearly absent among all other strains and controls (Figure 2A). A similar profile was shown for additional nine features depicted in the heatmaps of *S. aureus* JE2 (Figure 2A). They start to be detectable at ~ 5 h with increasing abundance towards the end of the measurement at 15 h. In contrast, the features remained at the baseline level for the rest of strains and for the control. Another example of *S. aureus* species-specific time profiles is shown in Figure 2B. Out of 19 features detected in both *S. aureus* strains JE2 and Cowan1, a relevant feature at m/z 101.06079 is shown for all biological replicates and controls (Figure 2B). Very similar to Figure 2A, this particular feature started to increase towards the end of the measurement and was only present in both *S. aureus* strains with a high signal intensity and nearly not detected in the other strains and controls. Figure S2 shows the heatmaps and/or representative specific features identified for the remaining species and strains. Unique features were assigned to each strain and species with the exception of *S. pneumoniae* TIGR4 for which no unique features were assigned, albeit its growth was confirmed by TL (See also Figure S1). Nevertheless, some features were present in *S. pneumoniae* TIGR4 whereas they were absent in the control (See also Figure S2E and Figure S2F).

Furthermore, we also compared the overlap of features detected using low-density culture (Table S1) versus using a high-saturated growth plate (Table S2). Only six species *S. pneumoniae*-specific features were found under both conditions (See also Figure S3).

Diverging metabolic trajectories of bacterial strains

Next, we investigated the evolution over time of the features produced by the different bacteria under investigation as they grew. Given the large number of features detected, we visualized our multivariate dataset using principal component analysis (PCA) and dendrogram trees to obtain clusters of the different bacterial strains at different stages of bacterial growth (Figure 3, See also Figure S4 and see also Figure S5). An initial separation of *S. pneumoniae* D39 from the other strains became apparent after 15 min of measurement (See also Figure S4). At the time point 7 h, a separation was noted for the *S. aureus* JE2 replicates. The *S. aureus* Cowan1 group started to drift apart from the controls at 10 h after growth. The best discrimination of the different groups was observed at 12 h as shown in the PCA and dendrogram tree in Figure 3. Except of *S. pneumoniae* TIGR4, all strains could be distinguished from the controls very clearly. Furthermore, it is well visible how Euclidean distance shortens as a function of growth time (See also Figure S5).

Measurement of clinical patient samples by SESI-HRMS

After assessing the quantitative and qualitative capabilities of our real-time analysis system to detect bacterial growth in enriched bacterial cultures, we tested the feasibility of such an approach for the direct analysis of a heterogeneous set of 17 clinical samples from 13 different patients derived from various origins including heart valves, skin, deep tissue, as well as foreign bodies such as pacemakers (Table 1). All clinical samples were initially analyzed by routine diagnostics and the etiological agents identified by MALDI-TOF. Most samples came from patients which underwent antibiotic therapy prior to SESI-HRMS measurement. Hence, for 10 out of the 17 clinical samples, no bacterial growth was detected by conventional growth on agar plates. For the remaining seven samples for which bacterial growth was detected, four were *S. aureus* positive and three grew *S. epidermidis* at the time of measurement by SESI-HRMS (Table 1). This is a typical problem encountered in clinics rendering the current culture-based microbiological diagnostics inefficient. Indeed, our clinical information confirmed that 11 out of 13 patients from this study were previously treated with different doses of antibiotics, and no bacterial growth could be detected at the sampling time for eight out of 13 of these patients (Table 1).

Despite these challenges, all samples obtained from patients were subjected to a targeted analysis whereby the specific features previously identified under high-density conditions were extracted from the clinical dataset. To then visualize this highly complex dataset, t-SNE analysis was performed (Figure 4). A clear cluster in the middle of the t-SNE space consisting of clinical samples from *S. aureus* (methicillin-susceptible, MSSA)

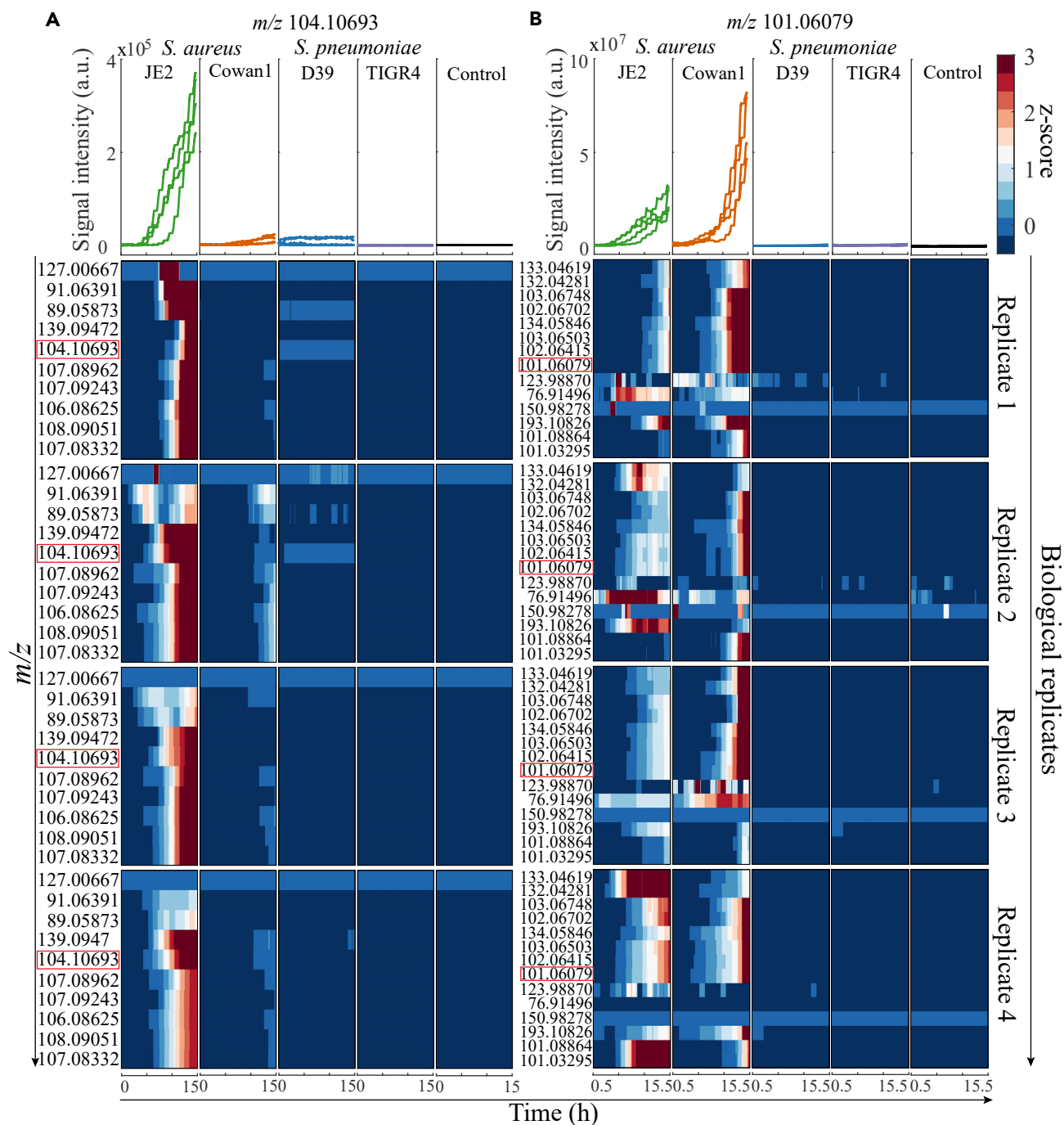


Figure 2. Specific time-dependent features detected during bacterial growth

(A) Example time trace of the positive ion at m/z 104.10693 (framed in red) unique to *S. aureus* JE2 is shown on top of the heatmaps consisting of total ten features (positive ions) unique to *S. aureus* JE2.

(B) Example time trace of the negative ion at m/z 101.06079 (framed in red) unique to the species *S. aureus* (i.e. present in both JE2 and Cowan1) is shown on top of the heatmaps consisting of total 14 features (negative ions) unique to species *S. aureus*. Real-time evolution of all features is shown over 15 h of measurement by SESI-HRMS for all four investigated strains ($n = 4$ biological replicates) and controls ($n = 4$). The color bar indicates the z-score values of absolute signal intensity for each feature, from low (dark blue) to increased signal intensity (dark red). See also Figures S2 and S3 and Tables S1 and S2.

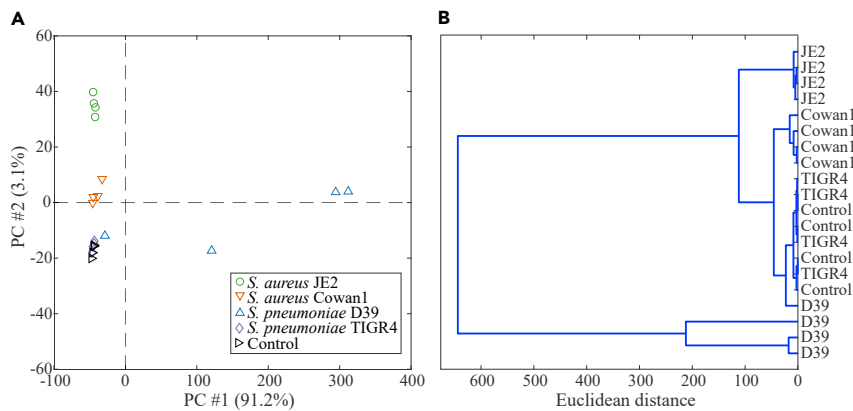


Figure 3. PCA score plot and dendrogram of PCA scores explaining 95% of variance illustrated at time point 12 h after the start of measurement

(A) PCA score plot of 1235 strain-specific features (positive and negative ions) at 12 h identified for high CFU cultures. (B) Dendrogram showing the detailed hierarchical relationship between bacterial species and strains at time point 12 h. See also [Figures S4](#) and [S5](#).

and *S. epidermidis* infections is visible. For these samples, growth of bacteria was confirmed *a posteriori* ([Table 1](#)). In addition, two clinical *S. aureus* samples (MRSA, further growth not confirmed) clustered at the bottom-right of the t-SNE space.

DISCUSSION

In this study, we showed that SESI-HRMS detects in real-time unique features of the human pathogens *S. aureus* and *S. pneumoniae* within minutes of growth on an agar plate. We obtained detectable features using bacterial cultures with less than 10^3 CFUs. Furthermore, a clear differentiation between these important two human bacterial pathogens was achieved, even within strains. Since bacterial numbers are often low in patient samples, especially if the patients already received antimicrobial therapy, this is of great importance for future diagnostics.

For any diagnostic method to be of clinical use, it requires to be sensitive and specific enough to enable meaningful further clinical decisions such as an accurate antibiotic treatment. A third dimension of crucial importance in diagnostics of suspected bacterial infection is time-to-response. A perfect diagnostic method should be sensitive enough to detect a positive sample during early phases of infection, selective enough to distinguish different species or strains, and should be fast and require little-to-no sample preparation. Currently, state-of-the-art DNA-based diagnostic methods for bacterial identification require just a single bacterial component to provide a positive response ([Clark Andrew et al., 2013](#)). However, limitations include that no differentiation between living and dead bacteria or a limited identification of antibiotic susceptibilities are possible. These limitations can seriously affect its clinical usefulness ([Vrioni et al., 2018](#)). On the other side, peptide profile identification by mass spectrometric methods can overcome these two noted limitations of DNA-based methods. However, this comes at the expense of requiring relatively lengthy pre-growing steps to enable active and sufficient bacterial cells to be detected by the MALDI-TOF system ([Buchan et al., 2012](#); [Kok et al., 2011](#); [Osthoff et al., 2017](#)).

The proposed mass spectrometric method lies somewhere in between these two techniques, hence overcoming some of their limitations. On the one hand, detectable features accumulate in the headspace of the specimen only if the bacteria replicate, hence are alive. On the other hand, the data presented in here suggest that bacterial loads in the order of 10^3 CFUs are enough to be detected within one hour by SESI-HRMS, well before sophisticated image analysis methods detect any indication of macroscopic bacterial growth which is the current gold standard in diagnostics. Moreover, the proposed approach analyzes features in real time, hence enables monitoring the blood agar plates directly as the bacteria grow. The real-time measurement of bacteria growth could potentially allow for a versatile diagnostic where physicians will have access to pathogen identification in real time with a high level of confidence. In addition, this provides a large automation potential as one can easily envisage multiplexing multiple dishes whereby an automatic valve would switch across samples to monitor their growth every few minutes.

Table 1. Clinical characteristics of patient samples analyzed by SESI-HRMS

Sample identifier	Clinical Microbiology	Growth parallel to SESI-HRMS	Sample type	Condition	Antibiotics prior sampling
1	Methicillin-resistant <i>Staphylococcus aureus</i> (MRSA)	no	Lung tissue	Pneumonia	yes
2	Methicillin-resistant <i>Staphylococcus aureus</i> (MRSA)	no	Blood	Bacteremia	not available
3	<i>Staphylococcus aureus</i> (MSSA)	no	Heart valve	Endocarditis	yes
4	<i>Staphylococcus aureus</i> (MSSA)	no	Heart valve	Endocarditis	yes
5	<i>Aggregatibacter</i> spp. <i>Actinomyces meyeri</i>	no	Lung tissue	Pneumonia with empyema	yes
6	<i>Staphylococcus aureus</i> (MSSA)	yes	Heart valve	Endocarditis	yes
7	<i>Staphylococcus aureus</i> (MSSA)	yes	Heart valve	Endocarditis	yes
8	<i>Staphylococcus aureus</i> (MSSA)	yes	Heart valve	Endocarditis	yes
9	<i>Staphylococcus aureus</i> (MSSA) <i>Staphylococcus lugdunensis</i> <i>Staphylococcus epidermidis</i>	yes	Nasal aspirate	Bacterial sinusitis	yes
10	<i>Staphylococcus epidermidis</i>	yes	Cardiac device	Pacemaker infection	no
11	<i>Staphylococcus epidermidis</i>	yes	Cardiac device	Pacemaker infection	no
12	<i>Staphylococcus epidermidis</i>	yes	Cardiac device	Pacemaker infection	no
13	not available	no	Cardiac device	Pacemaker infection	yes
14	<i>Staphylococcus aureus</i> (MSSA)	no	Cardiac device	Pacemaker infection	yes
15	<i>Streptococcus anginosus</i>	no	Cardiac device	Pleural empyema	no
16	<i>Parvimonas micra</i>	no	Lung tissue	Pleural empyema	yes
17	<i>Aggregatibacter</i> (<i>Haemophilus</i>) <i>aphrophilus</i>	no	Lung tissue	Thoracic hematoma	yes

Description of clinical microbiology, detected growth by SESI-HRMS, sample type, clinical condition and whether there was antibiotic treatment before analysis by SESI-HRMS.

Regarding the selectivity required to discriminate different pathogens, the high resolution of Orbitrap mass analyzers enables the separation of typically thousands of ions in the m/z range of 50–500, where most of the features from VOCs lie (Rochat, 2016). Such resolving power renders a very high specificity potential when it comes to distinguish specific metabolic patterns stemming from different microorganisms. In our case, hundreds of features were found to be unique to each species. For the first time, we showed here that such discrimination ability can go down to the strain level, reinforcing the notion that metabolomics is very well suited to capture such subtle heterogeneity as it provides a downstream read-out of genetic plus environmental factors (Choueiry et al., 2022; Johnson et al., 2016). The different environments between low- and high-CFU conditions may well explain the rather diverse metabolic signature observed under both conditions, leading to a modest overlap in the features detected under such different conditions.

Thus, overall SESI-HRMS identification of bacterial species by the present design suggests a high level of sensitivity and specificity, whereby already after 6 min, some strains, like *S. pneumoniae* D39, differ substantially from negative controls. The best separation was observed after 12 h, which can be notably quicker than the current MALDI-TOF identification procedures.

Proof-of-principle of the applicability of the method in a more realistic clinical context was also achieved by measuring clinical samples, including patient tissue and foreign material (e.g. pacemakers). This is one key advantage of this technique, as it requires no sample preparation, and therefore it is suitable for any solid or liquid specimen with a total analysis time of five–ten minutes to fingerprint the samples. In this study, 17 clinical samples from 13 different patients and from different origin were measured by SESI-HRMS. Following the standard procedure after a bacterial infection is diagnosed, those patients received antibiotics aiming to clear

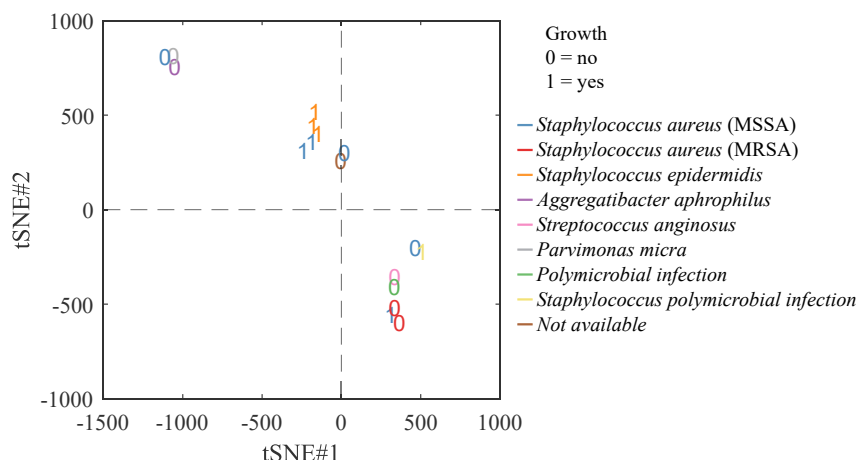


Figure 4. t-SNE analysis of clinical patient samples

Samples for which growth of the bacteria could be confirmed in parallel to SESI-HRMS measurement are represented as 1 = yes, whereas samples where no growth was observed are represented as 0 = no. The different colors indicate the causative bacterial strains responsible for the infection obtained in the sample withdrawn from patients. For details regarding the samples, refer to Table 1. MSSA = Methicillin-susceptible *Staphylococcus aureus*, MRSA = Methicillin-resistant *Staphylococcus aureus*.

the infection. This often interferes with diagnostics because bacteria do not grow anymore after antibiotic challenge as was the case at the time of sampling and analysis by SESI-HRMS. Four out of seven samples with an ongoing *S. aureus* infection and positive bacterial growth at the time of the analysis, clustered together in the t-SNE space (Figure 4). These results were obtained despite a low bacterial load in the clinical samples. Similar studies have been performed with technologies such as ion mobility spectrometry coupled to gas chromatography or multicapillary columns with various levels of sensitivity reported; however, these studies included the enrichment of bacteria in blood culture bottles or uptake of sample in transfer bags (Drees et al., 2019; Steppert et al., 2021), while in this study the samples were measured without any prior enrichment or preprocessing. While these results should be interpreted with caution, they clearly suggest that the proposed methodology for diagnostics in bacterial infections can be used with unprocessed clinical material.

In conclusion, we tested the concept of exploiting the fact that bacteria produce complex volatile metabolic mixtures as they proliferate. SESI-HRMS features a high gas-phase species' sensitivity and a great selectivity driven by the high-resolution of the mass analyzer. This was accomplished in real time, without any sample preparation. These characteristics allowed for the first time to monitor the kinetic profiles of hundreds of metabolic species emitted by *S. aureus* and *S. pneumoniae* as they grew on agar plates. These hundreds of features rendered highly specific signatures, which enabled distinguishing the samples even at the strain level. Finally, we scaled-up the concept to test the feasibility of evaluating clinical samples retrieved from patients with bacterial infections. The results showed that such samples can be fingerprinted within five minutes. Characteristic metabolic patterns emerged, suggesting the potential of such an approach to complement current diagnostic methods.

LIMITATIONS OF THE STUDY

While we showed that SESI-HRMS allows a rapid, sensitive, and selective discrimination of bacteria species down to a strain level and the feasibility to fingerprint clinical samples within five minutes, this study also comes with limitations that need to be addressed. One important limitation is the use of only Gram-positive bacteria. In addition, this study evaluated the identification of *Staphylococcus epidermidis* from clinical samples but not from *Streptococcus mitis* or other bacteria known for challenging identification. However, given the ability of this technique to identify unique features between two different strains of the same species, we believe this approach will allow for a more accurate determination of difficult-to-identify bacteria of clinical interest. Additionally, VOC libraries of relevant bacterial pathogens, as they are available for MALDI-TOF, need to be constructed in a follow-up work along with a machine learning classification algorithm to allow a prediction/ identification of the bacteria causing the infection. Such library will allow the identification of relevant VOCs which was not in the scope of the current study. Additionally, a very common

limitation on these types of devices and their application in the field are their high acquisition and maintenance costs. However, in comparison to a GC-MS setup for the purpose of clinical diagnostic, the SESI-HRMS design used in this study is comparable regarding their price. Nevertheless, the results obtained in this study and the application of the SESI-HRMS allow to consider an outlook with a simplified version of the proposed setup in which given a larger library of samples and algorithms for data analysis will facilitate a possible reduction in price. Finally, the number of samples and the single center nature represent an additional limitation inherent to the setup used in this study. The COVID-19 pandemic along with the direct measurement of samples from the operating room presented a technical challenge and did not allow to acquire a larger number of samples. Nevertheless, we believe that the advantages of a direct measurement of unprocessed samples directly from the operating room represented a unique opportunity to organize an interdisciplinary strategy and to evaluate the feasibility of the SESI-HRMS in the analysis of highly complex samples. Following this, benchmarking of the technology against MALDI-TOF and validation studies needs to be performed to evaluate the clinical utility of this method. All those steps are of pivotal importance to ensure correct antimicrobial therapy and optimal therapeutic outcome for the patient.

STAR★METHODS

Detailed methods are provided in the online version of this paper and include the following:

- KEY RESOURCES TABLE
- RESOURCE AVAILABILITY
 - Lead contact
 - Materials availability
 - Data and code availability
- EXPERIMENTAL MODEL AND SUBJECT DETAILS
 - Human clinical samples description and ethics
 - Bacterial strains and growth conditions
- METHOD DETAILS
 - Sampling of clinical patient material
 - Sample measurement with SESI-HRMS
 - Bacterial plate imaging
- QUANTIFICATION AND STATISTICAL ANALYSIS
 - SESI-HRMS data analysis
 - Time lapse image data analysis
- ADDITIONAL RESOURCES

SUPPLEMENTAL INFORMATION

Supplemental information can be found online at <https://doi.org/10.1016/j.isci.2022.105080>.

ACKNOWLEDGMENTS

We thank Prof. Dr. Sven Hammerschmidt from the Center for Functional Genomics of Microbes in Greifswald, Germany, for providing both *Streptococcus pneumoniae* strains D39 and TIGR4 (Jensch et al., 2010). We acknowledge the work from the medical personal from the University Hospital Zurich which facilitated the acquisition of the clinical samples and thank the patients for participating.

This work was supported by a grant from Fondation Botnar (Switzerland) and the Swiss National Science Foundation No. 320030_173168 and PCEGP3_181300 to P.S., the Swiss National Science Foundation grants nbr. 31003A_176252 to A.S.Z., as well as by the Clinical Research Priority Program of the University of Zurich Precision Medicine for Bacterial Infections to A.S.Z. and S.D.B. This work is part of the Zurich Exhalomics project under the umbrella of University Medicine Zurich/Hochschulmedizin Zürich.

AUTHOR CONTRIBUTIONS

Conception and Design, A.G.M., K.A., P.S., and A.S.Z.; Clinical Sample Collection and Processing, A.G.M., T.C.S., S.D.B., and A.S.Z. Data Analysis and interpretation, A.G.M., K.A., J.B., K.D.S., P.S., and A.S.Z. Manuscript Writing – Original Draft, A.G.M., K.A., P.S., and A.S.Z. Writing, Review & Editing, A.G.M., K.A., J.B., K.D.S., T.C.S., S.D.B., P.S., and A.S.Z. All authors read and approved the final manuscript.

DECLARATION OF INTERESTS

P.S. is cofounder of Deep Breath Initiative A.G. (Switzerland), which develops breath-based diagnostic tools. K.D.S. is consultant for Deep Breath Initiative A.G. (Switzerland).

Received: April 9, 2022

Revised: July 6, 2022

Accepted: August 31, 2022

Published: October 21, 2022

REFERENCES

- Allardyce, R.A., Hill, A.L., and Murdoch, D.R. (2006a). The rapid evaluation of bacterial growth and antibiotic susceptibility in blood cultures by selected ion flow tube mass spectrometry. *Diagn. Microbiol. Infect. Dis.* 55, 255–261. <https://doi.org/10.1016/j.diagmicrobio.2006.01.031>.
- Allardyce, R.A., Langford, V.S., Hill, A.L., and Murdoch, D.R. (2006b). Detection of volatile metabolites produced by bacterial growth in blood culture media by selected ion flow tube mass spectrometry (SIFT-MS). *J. Microbiol. Methods* 65, 361–365. <https://doi.org/10.1016/j.mimet.2005.09.003>.
- Altun, O., Botero-Kleiven, S., Carlsson, S., Ullberg, M., and Özenci, V. (2015). Rapid identification of bacteria from positive blood culture bottles by MALDI-TOF MS following short-term incubation on solid media. *J. Med. Microbiol.* 64, 1346–1352. <https://doi.org/10.1099/jmm.0.000168>.
- Ballabio, C., Cristoni, S., Puccio, G., Kohler, M., Sala, M.R., Brambilla, P., and Martinez-Lozano Sinues, P. (2014). Rapid identification of bacteria in blood cultures by mass-spectrometric analysis of volatiles. *J. Clin. Pathol.* 67, 743–746. <https://doi.org/10.1136/jclinpath-2014-202301>.
- Bär, J., Boumasmoud, M., Kouyou, R.D., Zinkernagel, A.S., and Vulin, C. (2020). Efficient microbial colony growth dynamics quantification with ColTapp, an automated image analysis application. *Sci. Rep.* 10, 16084. <https://doi.org/10.1038/s41598-020-72979-4>.
- Bean, H.D., Dimandja, J.M.D., and Hill, J.E. (2012). Bacterial volatile discovery using solid phase microextraction and comprehensive two-dimensional gas chromatography-time-of-flight mass spectrometry. *J. Chromatogr. B Analyt. Technol. Biomed. Life Sci.* 901, 41–46. <https://doi.org/10.1016/j.jchromb.2012.05.038>.
- Bean, H.D., Zhu, J., Sengle, J.C., and Hill, J.E. (2014). Identifying methicillin-resistant *Staphylococcus aureus* (MRSA) lung infections in mice via breath analysis using secondary electrospray ionization-mass spectrometry (SESI-MS). *J. Breath Res.* 8, 041001. <https://doi.org/10.1088/1752-7155/8/4/041001>.
- Bos, L.D.J., Sterk, P.J., and Schultz, M.J. (2013). Volatile metabolites of pathogens: a systematic Review. *PLoS Pathog.* 9, e1003311. <https://doi.org/10.1371/journal.ppat.1003311>.
- Buchan, B.W., Riebe, K.M., and Ledebner, N.A. (2012). Comparison of the MALDI Biotyper system using SepsiTyper specimen processing to routine microbiological methods for identification of bacteria from positive blood culture bottles. *J. Clin. Microbiol.* 50, 346–352. <https://doi.org/10.1128/jcm.05021-11>.
- Byun, H.-G., Persaud, K.C., and Pisanelli, A.M. (2010). Wound-state monitoring for burn patients using E-nose/SPME system. *ETRI J.* 32, 440–446. <https://doi.org/10.4218/etrij.10.0109.0300>.
- Casalnuovo, I., Di Piero, D., Coletta, M., and Di Francesco, P. (2006). Application of electronic noses for disease diagnosis and food spoilage detection. *Sensors* 6, 1428–1439.
- Cheng, D., Qiao, L., and Horvatovich, P. (2018). Toward spectral library-free matrix-assisted laser desorption/ionization time-of-flight mass spectrometry bacterial identification. *J. Proteome Res.* 17, 2124–2130. <https://doi.org/10.1021/acs.jproteome.8b00065>.
- Choi, S.-H., Dagher, M., Ruffin, F., Park, L.P., Sharma-Kuinkel, B.K., Souli, M., Morse, A.M., Eichenberger, E.M., Hale, L., Kohler, C., et al. (2021). Risk factors for recurrent *Staphylococcus aureus* bacteremia. *Clin. Infect. Dis.* 72, 1891–1899. <https://doi.org/10.1093/cid/ciaa801>.
- Choueiry, F., Xu, R., and Zhu, J. (2022). Adaptive metabolism of *Staphylococcus aureus* revealed by untargeted metabolomics. *J. Proteome Res.* 21, 470–481. <https://doi.org/10.1021/acs.jproteome.1c00797>.
- Clark, A.E., Kaleta, E.J., Arora, A., and Wolk, D.M. (2013). Matrix-Assisted laser desorption ionization-time of flight mass spectrometry: a fundamental shift in the routine practice of clinical microbiology. *Clin. Microbiol. Rev.* 26, 547–603. <https://doi.org/10.1128/CMR.00072-12>.
- Clark, C.M., Costa, M.S., Sanchez, L.M., and Murphy, B.T. (2018). Coupling MALDI-TOF mass spectrometry protein and specialized metabolite analyses to rapidly discriminate bacterial function. *Proc. Natl. Acad. Sci. USA* 115, 4981–4986. <https://doi.org/10.1073/pnas.1801247115>.
- Daulton, E., Wicaksono, A., Bechar, J., Covington, J.A., and Hardwicke, J. (2020). The detection of wound infection by ion mobility chemical analysis. *Biosensors* 10, E19. <https://doi.org/10.3390/bios10030019>.
- Drees, C., Vautz, W., Liedtke, S., Rosin, C., Althoff, K., Lippmann, M., Zimmermann, S., Legler, T.J., Yildiz, D., Perl, T., and Kunze-Szikszay, N. (2019). GC-IMS headspace analyses allow early recognition of bacterial growth and rapid pathogen differentiation in standard blood cultures. *Appl. Microbiol. Biotechnol.* 103, 9091–9101. <https://doi.org/10.1007/s00253-019-10181-x>.
- Gardner, J.W., and Bartlett, P.N. (1994). A brief history of electronic noses. *Sensor. Actuator. B Chem.* 18, 210–211. [https://doi.org/10.1016/0925-4005\(94\)87085-3](https://doi.org/10.1016/0925-4005(94)87085-3).
- Griffiths, J. (2008). A brief history of mass spectrometry. *Anal. Chem.* 80, 5678–5683. <https://doi.org/10.1021/ac8013065>.
- Henriques-Normark, B., and Normark, S. (2010). Commensal pathogens, with a focus on *Streptococcus pneumoniae*, and interactions with the human host. *Exp. Cell Res.* 316, 1408–1414. <https://doi.org/10.1016/j.yexcr.2010.03.003>.
- Jensch, I., Gámez, G., Rothe, M., Ebert, S., Fulde, M., Somplatzki, D., Bergmann, S., Petruschka, L., Rohde, M., Nau, R., and Hammerschmidt, S. (2010). PavB is a surface-exposed adhesin of *Streptococcus pneumoniae* contributing to nasopharyngeal colonization and airways infections. *Mol. Microbiol.* 77, 22–43. <https://doi.org/10.1111/j.1365-2958.2010.07189.x>.
- Johnson, C.H., Ivanisevic, J., and Siuzdak, G. (2016). Metabolomics: beyond biomarkers and towards mechanisms. *Nat. Rev. Mol. Cell Biol.* 17, 451–459. <https://doi.org/10.1038/nrm.2016.25>.
- Kaeslin, J., Micic, S., Weber, R., Müller, S., Perkins, N., Berger, C., Zenobi, R., Bruderer, T., and Moeller, A. (2021). Differentiation of cystic fibrosis-related pathogens by volatile organic compound analysis with secondary electrospray ionization mass spectrometry. *Metabolites* 11, 773. <https://doi.org/10.3390/metabo11110773>.
- Keller, B.O., Sui, J., Young, A.B., and Whittall, R.M. (2008). Interferences and contaminants encountered in modern mass spectrometry. *Anal. Chim. Acta* 627, 71–81. <https://doi.org/10.1016/j.aca.2008.04.043>.
- Kind, T., and Fiehn, O. (2007). Seven Golden Rules for heuristic filtering of molecular formulas obtained by accurate mass spectrometry. *BMC Bioinf.* 8, 105. <https://doi.org/10.1186/1471-2105-8-105>.
- Kok, J., Thomas, L.C., Olma, T., Chen, S.C.A., and Iredell, J.R. (2011). Identification of bacteria in blood culture broths using matrix-assisted laser desorption-ionization SepsiTyper™ and time of flight mass spectrometry. *PLoS One* 6, e23285. <https://doi.org/10.1371/journal.pone.0023285>.
- Kumar, A., Roberts, D., Wood, K.E., Light, B., Parrillo, J.E., Sharma, S., Suppes, R., Feinstein, D., Zanotti, S., Taiberg, L., et al. (2006). Duration of hypotension before initiation of effective antimicrobial therapy is the critical determinant of survival in human septic shock. *Crit. Care Med.* 34,

1589–1596. <https://doi.org/10.1097/01.Ccm.0000217961.75225.E9>.

- Kyaw, M.H., Rose, C.E., Jr., Fry, A.M., Singleton, J.A., Moore, Z., Zell, E.R., and Whitney, C.G.; Active Bacterial Core Surveillance Program of the Emerging Infections Program Network (2005). The influence of chronic illnesses on the incidence of invasive pneumococcal disease in adults. *J. Infect. Dis.* 192, 377–386. <https://doi.org/10.1086/431521>.
- Lee, J.H.J., and Zhu, J. (2020). Optimizing secondary electrospray ionization high-resolution mass spectrometry (SESI-HRMS) for the analysis of volatile fatty acids from gut microbiome. *Metabolites* 10, 351. <https://doi.org/10.3390/metabo10090351>.
- Li, H., Xu, M., and Zhu, J. (2019). Headspace gas monitoring of gut microbiota using targeted and globally optimized targeted secondary electrospray ionization mass spectrometry. *Anal. Chem.* 91, 854–863. <https://doi.org/10.1021/acs.analchem.8b03517>.
- Li, H., and Zhu, J. (2018). Differentiating antibiotic-resistant *Staphylococcus aureus* using secondary electrospray ionization tandem mass spectrometry. *Anal. Chem.* 90, 12108–12115. <https://doi.org/10.1021/acs.analchem.8b03029>.
- Lodise, T.P., McKinnon, P.S., Swiderski, L., and Rybak, M.J. (2003). Outcomes analysis of delayed antibiotic treatment for hospital-acquired *Staphylococcus aureus* bacteremia. *Clin. Infect. Dis.* 36, 1418–1423. <https://doi.org/10.1086/375057>.
- Lowy, F.D. (1998). *Staphylococcus aureus* infections. *N. Engl. J. Med.* 339, 520–532. <https://doi.org/10.1056/nejm199808203390806>.
- Martínez-Lozano, P., Rus, J., Fernández de la Mora, G., Hernández, M., and Fernández de la Mora, J. (2009). Secondary electrospray ionization (SESI) of ambient vapors for explosive detection at concentrations below parts per trillion. *J. Am. Soc. Mass Spectrom.* 20, 287–294. <https://doi.org/10.1016/j.jasms.2008.10.006>.
- Nomura, F., Tsuchida, S., Murata, S., Satoh, M., and Matsushita, K. (2020). Mass spectrometry-based microbiological testing for blood stream infection. *Clin. Proteomics* 17, 14. <https://doi.org/10.1186/s12014-020-09278-7>.
- Opota, O., Jatou, K., and Greub, G. (2015). Microbial diagnosis of bloodstream infection: towards molecular diagnosis directly from blood. *Clin. Microbiol. Infect.* 21, 323–331. <https://doi.org/10.1016/j.cmi.2015.02.005>.
- Osthoff, M., Gürtler, N., Bassetti, S., Balestra, G., Marsch, S., Pargger, H., Weisser, M., and Egli, A. (2017). Impact of MALDI-TOF-MS-based identification directly from positive blood cultures on patient management: a controlled clinical trial. *Clin. Microbiol. Infect.* 23, 78–85. <https://doi.org/10.1016/j.cmi.2016.08.009>.
- Paul, M., Kariv, G., Goldberg, E., Raskin, M., Shaked, H., Hazzan, R., Samra, Z., Paghis, D., Bishara, J., and Leibovici, L. (2010). Importance of appropriate empirical antibiotic therapy for methicillin-resistant *Staphylococcus aureus* bacteraemia. *J. Antimicrob. Chemother.* 65, 2658–2665. <https://doi.org/10.1093/jac/dkq373>.
- Rasmussen, R.V., Fowler, V.G., Jr., Skov, R., and Bruun, N.E. (2010). Future challenges and treatment of *Staphylococcus aureus* bacteremia with emphasis on MRSA. *Future Microbiol.* 6, 43–56. <https://doi.org/10.2217/fmb.10.155>.
- Ratiu, I.A., Ligor, T., Bocos-Bintintan, V., Szeliga, J., Machała, K., Jackowski, M., and Buszewski, B. (2019). GC-MS application in determination of volatile profiles emitted by infected and uninfected human tissue. *J. Breath Res.* 13, 026003. <https://doi.org/10.1088/1752-7163/aa7f08>.
- Rochat, B. (2016). From targeted quantification to untargeted metabolomics: why LC-high-resolution-MS will become a key instrument in clinical labs. *TrAC, Trends Anal. Chem.* 84, 151–164. <https://doi.org/10.1016/j.trac.2016.02.009>.
- Roine, A., Saviak, T., Kumpulainen, P., Karjalainen, M., Tuokko, A., Aittoniemi, J., Vuento, R., Lekkala, J., Lehtimäki, T., Tammela, T.L., and Oksala, N.K.J. (2014). Rapid and accurate detection of urinary pathogens by mobile IMS-based electronic nose: a proof-of-principle study. *PLoS One* 9, e114279. <https://doi.org/10.1371/journal.pone.0114279>.
- Sahota, A.S., Gowda, R., Arasaradnam, R.P., Daulton, E., Savage, R.S., Skinner, J.R., Adams, E., Ward, S.A., and Covington, J.A. (2016). A simple breath test for tuberculosis using ion mobility: a pilot study. *Tuberculosis* 99, 143–146. <https://doi.org/10.1016/j.tube.2016.05.005>.
- Schlosser, A., and Volkmer-Engert, R. (2003). Volatile polydimethylcyclsiloxanes in the ambient laboratory air identified as source of extreme background signals in nano-electrospray mass spectrometry. *J. Mass Spectrom.* 38, 523–525. <https://doi.org/10.1002/jms.465>.
- Sethi, S., Nanda, R., and Chakraborty, T. (2013). Clinical application of volatile organic compound analysis for detecting infectious diseases. *Clin. Microbiol. Rev.* 26, 462–475. <https://doi.org/10.1128/CMR.00020-1310.1088/1752-7155/6/2/027108>.
- Singhal, N., Kumar, M., Kanaujia, P.K., and Virdi, J.S. (2015). MALDI-TOF mass spectrometry: an emerging technology for microbial identification and diagnosis. *Front. Microbiol.* 6, 791. <https://doi.org/10.3389/fmicb.2015.00791>.
- Slade, E.A., Thorn, R.M.S., Lovering, A.M., Young, A., and Reynolds, D.M. (2017). In vitro discrimination of wound-associated bacteria by volatile compound profiling using selected ion flow tube-mass spectrometry. *J. Appl. Microbiol.* 123, 233–245. <https://doi.org/10.1111/jam.13473>.
- Steffert, I., Schönfelder, J., Schultz, C., and Kuhlmeier, D. (2021). Rapid in vitro differentiation of bacteria by ion mobility spectrometry. *Appl. Microbiol. Biotechnol.* 105, 4297–4307. <https://doi.org/10.1007/s00253-021-11315-w>.
- Tejero Rioseras, A., Garcia Gomez, D., Ebert, B.E., Blank, L.M., Ibañez, A.J., and Sinues, P.M.L. (2017). Comprehensive real-time analysis of the yeast volatiles. *Sci. Rep.* 7, 14236. <https://doi.org/10.1038/s41598-017-14554-y>.
- Thomas, A.N., Riazanskaia, S., Cheung, W., Xu, Y., Goodacre, R., Thomas, C.L.P., Baguneid, M.S., and Bayat, A. (2010). Novel noninvasive identification of biomarkers by analytical profiling of chronic wounds using volatile organic compounds. *Wound Repair Regen.* 18, 391–400. <https://doi.org/10.1111/j.1524-475X.2010.00592.x>.
- Vandamme, P., Pot, B., Gillis, M., de Vos, P., Kersters, K., and Swings, J. (1996). Polyphasic taxonomy, a consensus approach to bacterial systematics. *Microbiol. Rev.* 60, 407–438. <https://doi.org/10.1128/mr.60.2.407-438.1996>.
- Vrioni, G., Tsiamis, C., Oikonomidis, G., Theodoridou, K., Kapsimali, V., and Tsakris, A. (2018). MALDI-TOF mass spectrometry technology for detecting biomarkers of antimicrobial resistance: current achievements and future perspectives. *Ann. Transl. Med.* 6, 240.
- Yarza, P., Yilmaz, P., Pruesse, E., Glöckner, F.O., Ludwig, W., Schleifer, K.H., Whitman, W.B., Euzéby, J., Amann, R., and Rosselló-Móra, R. (2014). Uniting the classification of cultured and uncultured bacteria and archaea using 16S rRNA gene sequences. *Nat. Rev. Microbiol.* 12, 635–645. <https://doi.org/10.1038/nrmicro3330>.
- Zhu, J., Bean, H.D., Kuo, Y.-M., and Hill, J.E. (2010). Fast detection of volatile organic compounds from bacterial cultures by secondary electrospray ionization-mass spectrometry. *J. Clin. Microbiol.* 48, 4426–4431. <https://doi.org/10.1128/JCM.00392-10>.
- Zhu, J., Bean, H.D., Wargo, M.J., Leclair, L.W., and Hill, J.E. (2013a). Detecting bacterial lung infections: in vivo evaluation of in vitro volatile fingerprints. *J. Breath Res.* 7, 016003. <https://doi.org/10.1088/1752-7155/7/1/016003>.
- Zhu, J., and Hill, J.E. (2013). Detection of *Escherichia coli* via VOC profiling using secondary electrospray ionization-mass spectrometry (SESI-MS). *Food Microbiol.* 34, 412–417. <https://doi.org/10.1016/j.fm.2012.12.008>.
- Zhu, J., Bean, H.D., Jiménez-Díaz, J., and Hill, J.E. (2013b). Secondary electrospray ionization-mass spectrometry (SESI-MS) breathprinting of multiple bacterial lung pathogens, a mouse model study. *J. Appl. Physiol.* 114, 1544–1549. <https://doi.org/10.1152/jappphysiol.00099.2013>.
- Zhu, J., Jiménez-Díaz, J., Bean, H.D., Daphtary, N.A., Aliyeva, M.I., Lundblad, L.K.A., and Hill, J.E. (2013c). Robust detection of *P. aeruginosa* and *S. aureus* acute lung infections by secondary electrospray ionization-mass spectrometry (SESI-MS) breathprinting: from initial infection to clearance. *J. Breath Res.* 7, 037106. <https://doi.org/10.1088/1752-7155/7/3/037106>.

STAR★METHODS

KEY RESOURCES TABLE

REAGENT or RESOURCE	SOURCE	IDENTIFIER
Bacterial and virus strains		
<i>Staphylococcus aureus</i> strain JE2	NARSA collection	NR-46543
<i>Staphylococcus aureus</i> strain COWAN I	ATCC	ATCC 12598
<i>Streptococcus pneumoniae</i> strain D39	Jensch et al. (2010)	Prof. Sven Hammerschmidt
<i>Streptococcus pneumoniae</i> strain TIGR4	Jensch et al. (2010)	Prof. Sven Hammerschmidt
Biological samples		
Patient material: tissue, blood, pus, foreign material	University Hospital Zurich	Within clinical studies: Vascular Graft Cohort study (VASGRA; KEK-2012-0583), the Endovascular and Cardiac Valve Infection Registry (ENVALVE; BASEC 2017-01140), the Prosthetic Joint Infection Cohort (Balgrist, BASEC 2017-01458), and BacVivo (BASEC 2017-02225)
Chemicals, peptides, and recombinant proteins		
Water with 0.1% (v/v) Formic acid	Merck	Cat#159013
Deposited data		
Raw and Analyzed data	MetaboLights	MetaboLights: MTBLS5085
Software and algorithms		
Auto Click Typer version 2.0	VCL Examples	https://auto-click-typer.software.informer.com/2.0/
MATLAB version 2021b	MathWorks	https://ch.mathworks.com/products/matlab.html
Coltapp version 1.0	MathWorks	Bär et al. (2020)
Thermo Exactive Plus Tune software version 2.9	Thermo Fisher Scientific	Thermo Fisher Scientific
Other		
TaperTip silica capillary emitter	New Objective, USA	www.mswil.com

RESOURCE AVAILABILITY

Lead contact

Further information and requests for resources and reagents should be directed to and will be fulfilled by the lead contact, Pablo Sinues (pablo.sinues@unibas.ch).

Materials availability

This study did not generate new unique reagents, bacterial strains or plasmids.

Data and code availability

- RAW files obtained from real-time mass spectrometric measurements have been deposited at MetaboLights: [MTBLS5085](#).
- This paper does not report original code.
- Any additional information required to reanalyze the data reported in this paper is available from the [lead contact](#) upon reasonable request.

EXPERIMENTAL MODEL AND SUBJECT DETAILS

Human clinical samples description and ethics

For this study, 17 samples from 13 patients with vascular graft /endovascular infections, infective endocarditis, bone and prosthetic joint infections and any other infections were collected during the time period of November 2020 to May 2021 in the framework of the Vascular Graft Cohort study (VASGRA; KEK-2012-0583), the Endovascular and Cardiac Valve Infection Registry (ENVALVE; BASEC 2017-01140), the Prosthetic Joint Infection Cohort (Balgrist, BASEC 2017-01458), and BacVivo (BASEC 2017-02225), respectively. The study was approved by the local ethics committee of the Canton of Zurich, Switzerland. Information regarding sex and demographics of the patients is not deemed necessary for the analysis and conclusions obtained in this study and in order to improve the anonymity of the patients it is not provided. A more detailed description regarding the type of sample, etiological agent and antibiotic treatment prior to the analysis can be found in [Table 1](#).

Bacterial strains and growth conditions

S. aureus (JE2 and Cowan1) and *S. pneumoniae* (D39 and TIGR4) were initially cultivated axenically from glycerol stocks on Columbia agar plates with 5% sheep blood (BioMérieux) at 37°C and 5% CO₂ for ~15 to 16 h. Two different sets of experiments were performed with each strain. The first experiment consisted of plating a high-density culture (i.e. high CFUs) by performing a subculture on a fresh blood agar plate directly from the overnight plate (14 to 16 h). In the second experiment, the initial overnight culture in agar was resuspended in PBS and diluted to obtain a low number of CFUs (i.e. low CFUs) ranging from ~140 to ~2000 CFUs per plate.

METHOD DETAILS

Sampling of clinical patient material

Clinical samples were obtained from patients with bacterial infections requiring surgery with a total time from sample transfer from the operating room to the SESI-HRMS set up of approximately 30 min. The description of the different clinical samples used in this study such as origin, identified bacterial pathogen, and antibiotic treatment prior to sampling is depicted in [Table 1](#). The processing of the patient material depended on the characteristics of the sample. To verify the growth of bacteria from these samples, the clinical sample obtained directly from the operating room was immediately transferred to a BSL-2 laboratory and divided into two parts, one for direct and raw measurement by SESI-HRMS and one for colony plating and quantification. In short, the patient's material part designated for SESI-HRMS measurement was directly transferred to a BSL-2 laboratory equipped with a high-resolution mass spectrometer (Exactive Plus, Thermo Fisher Scientific, Germany) with an ion-source (Super SESI, FIT, Spain) connected to a custom-made airtight sample box. The raw, unprocessed sample was placed inside the airtight box and measured as described in the section "[Sample measurement with SESI-HRMS](#)". For bacterial recovery and quantification, samples such as skin, heart valves and soft tissues were processed by disrupting the tissue using a tissue lyser (Qiagen TissueLyser, vibration frequency of 30/s for 10 min). For foreign material such as pacemakers, the processing involved an initial sonication step of 5 min using a sonicator bath (Ultrasonic bath XUBA3, Grant) in sterile PBS. Following these two initial steps, the remaining processing protocol was the same for all samples. The resulting suspension was washed twice with sterile PBS to remove traces of antibiotics from the sample and a final step with sterile milliQ water was used to lyse the eukaryotic cells. The sample was then serially diluted in sterile milliQ water, plated on blood agar plate and incubated at 37°C and 5% CO₂ for 24 h to monitor for growth. In total, 17 clinical samples from 13 different patients were used for analysis.

Sample measurement with SESI-HRMS

The experimental set-up consisted of a custom-made plexiglass box (dimensions: width 120 mm, length 120 mm, height 100 mm) with an airtight closing mechanism which was directly connected to an ion source (Super SESI, FIT, Spain) coupled to a high-resolution mass spectrometer (Exactive Plus, Thermo Fisher Scientific, Germany). The sample (bacteria plate or clinical patient material) was placed inside the plexiglass box which was heated at 37°C in a water bath. A mass flow controller was coupled to the box on the opposite side of the SESI-HRMS via PTFE - tubes and ensured a constant medical grade air supply through the system at a flow rate of 0.5 L/min and carried the VOCs emitted by the bacterial cultures or from the clinical material towards the SESI-HRMS. Mass spectral analysis of bacteria plates was conducted over a period of ~15 h and for 5 min in case of clinical samples. An automated switch system (Auto Click Typer version 2.0)

allowed to alter between positive and negative ionization mode every 30 min when measurements were conducted for ~15h. In addition, a high-resolution camera was placed above the box and was triggered as described in the “bacterial plate imaging” section of the [STAR Methods](#). In total, 36 bacterial plates measurements were performed whereby for both conditions (high-density and low CFUs) a total of 16 measurements were conducted each ($n = 4$ biological replicates per strain) along with measurements of empty blood agar plates which served as control measures ($n = 4$) for both CFU conditions. Furthermore, a total of 17 clinical samples from 13 different patients were analyzed by SESI-HRMS.

To generate the electrospray in the SESI, a 20- μm ID TaperTip silica capillary emitter (New Objective, USA) and a solution of 0.1% formic acid in water were used. The pressure of the SESI solvent environment was set to 1.3 bar. Temperature of the ionization chamber and the sampling line was set to 90°C and 130°C respectively. The voltage of the electrospray was set to 3.7 kV in positive and 3 kV in negative ionization mode. The sheath gas flow rate was set to 10, capillary temperature was 320°C and S-lens RF level 50.0.

Mass spectra were acquired via Thermo Exactive Plus Tune software (version 2.9) in full scan mode (scan range 50–500 m/z , polarity positive or negative, microscan number 10, ACG target 10^6 , maximum injection time 50 ms) at a resolving power of 140000 at m/z 200. The system was calibrated on a regular basis before the measurements externally and internally by using common background contaminants as lock masses in the respective polarity ([Keller et al., 2008](#); [Schlosser and Volkmer-Engert, 2003](#))

Bacterial plate imaging

Simultaneously as the plate was analyzed for the production of VOCs by SESI-HRMS, a TL imaging experiment was performed using a high-resolution camera (Cannon EOS 1200D reflex) triggered every 10 min by an Arduino Uno board (Arduino) to capture images of the plate inside the box to visually document bacterial growth ([Bär et al., 2020](#)). To verify the growth of the bacteria on the plate, TL measurement was conducted until ~40 h for specific replicates.

QUANTIFICATION AND STATISTICAL ANALYSIS

SESI-HRMS data analysis

Data analysis was performed using MATLAB (version 2021b, MathWorks Inc., USA). Raw mass spectra files were accessed via inhouse C# console apps based on Thermo Fisher Scientific’s RawFileReader (version 5.0.0.38). The MATLAB functions, *ksdensity* and *mspeaks* were applied to generate the final list of features. In short, *ksdensity* was used in a first step to appropriately bin the centroid peak list from each scan of all files to generate a further peak list. In a second step, the *mspeaks* function was applied to extract relevant features via specification of the HEIGHTFILTER criteria to define the minimum permissible height for all reported peaks and to remove the others from the output feature list. For some peaks (i.e. m/z 59-60 in negative mode and m/z 257 in positive mode) we observed noisy interferences from the mass spectrometer (detected by visual inspection of the output plots of the *mspeaks* function). Therefore, these m/z were completely excluded from further analysis. As a result, a data matrix of total 571 files (165551 time points) \times 3439 mass spectral features in positive mode and 571 files (165275 time points) \times 1033 mass spectral features in negative mode was obtained. Signal intensity time traces of all features were then computed and smoothed (moving mean; span = 300) for visualization purposes. The mean Area Under the Curve (mAUC) of the time traces ($n = 4$ replicates per strain) was calculated by interpolating the data every 0.01h. To identify features, unique to a particular bacterial strain, two criteria were defined; first criteria kept only features with a \log_2 fold change (FC) ≥ 2 in mAUC of a particular strain compared to the mAUC of the control and 2nd criteria required a \log_2 FC ≥ 4 in mAUC of the particular strain compared to the averaged mAUC of the other investigated strains. Furthermore, species specific time traces were identified, meaning that they had to be present in both *S. pneumoniae* strains (D39 and TIGR4) or both *S. aureus* strains (JE2 and Cowan1). Therefore three criteria were defined: first criteria kept only features with a \log_2 FC ≥ 2 in mAUC in both strains of a particular species compared to the mAUC of the control; 2nd criteria defined to only consider the features further if within one species the respective strains had at least a mAUC of 30% of the mAUC of the other strain under the respective species to avoid features to be selected which tended to be rather present in one strain and not in both; 3rd criteria considered only features which showed a \log_2 FC ≥ 4 in average mAUC of the two strains of one species compared to the average mAUC of the two strains of the other species and vice versa. In a next step the time traces of features unique for the different strains and species were auto scaled (z-score), subjected to a hierarchical cluster tree (Ward method; Euclidean distance) and visualized as heat maps showing the evolution of the features over time. Principal

Component Analysis (PCA) of 5th – root transformed data matrix and a hierarchical binary cluster tree (Ward Method; Euclidean distance) were used to visually discriminate the different bacterial strains at distinctive time points over ~15 h.

Clinical samples were analyzed using a targeted approach, where unique positive and negative time traces of features previously identified for the different strains under high density CFU condition were directly extracted from the clinical samples raw data using in-house C# console app based on RawFileReader which resulted in a data matrix of 17 × 1269 (samples × mass spectral features). We then performed t-distributed stochastic neighbor embedding (t-SNE) to visualize this highly complex and exploratory dataset.

For all features, molecular formulae were assigned based on accurate mass by using the “seven golden rules” (Kind and Fiehn, 2007), considering the elements C, H, N, O, P and S and the adducts [M + H], [M - H₂O + H], [M + NH₄], [M - NH₃ + H], [M + Na] in positive mode and [M - H], [M - Na], [M - H₂O - H], [M + NH₃ - H], [M - NH₄] in negative ionization mode.

Time lapse image data analysis

Simultaneously to the SESI-HRMS measurement, bacterial growth on agar was verified and quantified by time lapse imaging. The acquired TL images were analyzed with a custom extension for ColTapp software (Bär et al., 2020) to quantify the bacterial growth as changes in pixel intensity over time. As the visual growth pattern of *S. aureus* and *S. pneumoniae* are distinct, different image analysis pipelines were utilized. For *S. aureus*, images were transformed to grayscale by selecting the green channel of the Red Green Blue (RGB) image. Then, a subsequent top-hat filtering using a disk-shaped structuring element with a radius of 65 pixel was performed to reduce lighting heterogeneity. For *S. pneumoniae*, the RGB images were transformed to YIQ color space, subset to the I channel only and the complement image calculated. A gaussian filter with a kernel of 10 pixel was applied to the first image of the TL series to generate an empty background image which then was subtracted from each other image in the TL series. These steps achieved comparable lighting heterogeneity correction as with top-hat filtering for *S. aureus*.

The following steps were the same for both species: the corrected grayscale images were subset to include only the area within plate boundaries. Then, min-max scaling with [0, 0.7] as range was applied to the pixel intensities. Finally, the sum of all pixel intensities was divided by the sum of pixels to derive a normalized intensity value per time point of a TL image series.

ADDITIONAL RESOURCES

This work used clinical material from patients recruited from the following clinical cohorts for the identification of bacterial presence by SESI-MS: Vascular Graft Cohort study (VASGRA; KEK-2012-0583), [ClinicalTrials.gov](https://clinicaltrials.gov/ct2/show/NCT01821664) Identifier: NCT01821664, <https://clinicaltrials.gov/ct2/show/NCT01821664>. The Endovascular and Cardiac Valve Infection Registry (ENVALVE; BASEC 2017-01140), URL: <https://www.usz.ch/en/clinic/infectiology/research/endovascular-infections-envalve-cohort-study/>. The Prosthetic Joint Infection Cohort (Balgrist, BASEC 2017-01458) and BacVivo (BASEC 2017-02225). <https://www.bacvivo.uzh.ch/en/aboutus.html>.